CHALMERS
UNIVERSITY OF TECHNOLOGY

Avoiding CO2 capture effort and cost for negative CO2 emissions using industrial waste in chemical-looping combustion/gasification of biomass

Citation for the original published paper (version of record):
Moldenhauer, P., Linderholm, C., Rydén, M. et al (2020). Avoiding CO2 capture effort and cost for negative CO2 emissions using industrial waste in chemical-looping combustion/gasification of biomass. Mitigation and Adaptation Strategies for Global Change, 25(1): 1-24. http://dx.doi.org/10.1007/s11027-019-9843-2

Mitigation and Adaptation Strategies for Global Change
https://doi.org/10.1007/s11027-019-9843-2

ORIGINAL ARTICLE

Avoiding CO_2 capture effort and cost for negative CO_2 emissions using industrial waste in chemical-looping combustion/gasification of biomass

Patrick Moldenhauer[1] · Carl Linderholm[1] · Magnus Rydén[1] · Anders Lyngfelt[1]

Received: 15 August 2018 / Accepted: 16 January 2019/Published online: 15 March 2019

Abstract

Chemical-looping combustion (CLC) is a combustion process with inherent separation of carbon dioxide (CO_2), which is achieved by oxidizing the fuel with a solid oxygen carrier rather than with air. As fuel and combustion air are never mixed, no gas separation is necessary and, consequently, there is no direct cost or energy penalty for the separation of gases. The most common form of design of chemical-looping combustion systems uses circulating fluidized beds, which is an established and widely spread technology. Experiments were conducted in two different laboratory-scale CLC reactors with continuous fuel feeding and nominal fuel inputs of 300 W_{th} and 10 kW_{th}, respectively. As an oxygen carrier material, ground steel converter slag from the Linz–Donawitz process was used. This material is the second largest flow in an integrated steel mill and it is available in huge quantities, for which there is currently limited demand. Steel converter slag consists mainly of oxides of calcium (Ca), magnesium (Mg), iron (Fe), silicon (Si), and manganese (Mn). In the 300 W unit, chemical-looping combustion experiments were conducted with model fuels syngas (50 vol% hydrogen (H_2) in carbon monoxide (CO)) and methane (CH_4) at varied reactor temperature, fuel input, and oxygen-carrier circulation. Further, the ability of the oxygen-carrier material to release oxygen to the gas phase was investigated. In the 10 kW unit, the fuels used for combustion tests were steam-exploded pellets and wood char. The purpose of these experiments was to study more realistic biomass fuels and to assess the lifetime of the slag when employed as oxygen carrier. In addition, chemical-looping gasification was investigated in the 10 kW unit using both steam-exploded pellets and regular wood pellets as fuels. In the 300 W unit, up to 99.9% of syngas conversion was achieved at 280 kg/MW_{th} and 900 °C, while the highest conversion achieved with methane was 60% at 280 kg/MW_{th} and 950 °C. The material's ability to release oxygen to the gas phase, i.e., CLOU property, was developed during the initial hours with fuel operation and the activated material released 1–2 vol% of O_2

✉ Patrick Moldenhauer
patrick.moldenhauer@chalmers.se

[1] Division of Energy Technology, Chalmers University of Technology, 412 96 Gothenburg, Sweden

into a flow of argon between 850 and 950 °C. The material's initial low density decreased somewhat during CLC operation. In the 10 kW, CO_2 yields of 75–82% were achieved with all three fuels tested in CLC conditions, while carbon leakage was very low in most cases, i.e., below 1%. With wood char as fuel, at a fuel input of 1.8 kW_{th}, a CO_2 yield of 92% could be achieved. The carbon fraction of C_2-species was usually below 2.5% and no C_3-species were detected. During chemical-looping gasification investigation a raw gas was produced that contained mostly H_2. The oxygen carrier lifetime was estimated to be about 110–170 h. However, due to its high availability and potentially low cost, this type of slag could be suitable for large-scale operation. The study also includes a discussion on the potential advantages of this technology over other technologies available for Bio-Energy Carbon Capture and Storage, BECCS. Furthermore, the paper calls for the use of adequate policy instruments to foster the development of this kind of technologies, with great potential for cost reduction but presently without commercial application because of lack of incentives.

Keywords Chemical-looping combustion (CLC) · Chemical-looping gasification (CLG) · Biomass · Steel converter slag (LD slag) · Bio-energy carbon capture and storage (BECCS) · Negative CO2 emissions · Fluidized bed combustion

1 Introduction

1.1 Chemical-looping combustion and chemical-looping gasification

Figure 1 shows illustrations of the chemical-looping combustion and chemical-looping gasification principles

Chemical-looping combustion (CLC) is a carbon-capture technology with a potential to drastically reduce the cost of carbon dioxide (CO_2) sequestration. The most common adaptation of chemical-looping combustion is based on two interconnected, chemical reactors: in the air reactor (AR), air is used to oxidize a solid oxygen-carrier, and in the fuel reactor (FR), fuel is added and oxidized by the oxygen carrier, which, in turn, is reduced. In this way, the combustion products are not diluted with nitrogen and, after condensation of steam, the fuel-reactor flue gas ideally consists of pure CO_2. In contrast to other carbon-capture technologies, such as absorption or adsorption of CO_2 or oxyfuel combustion, there is no direct energy penalty for gas separation associated with chemical-looping combustion. General information

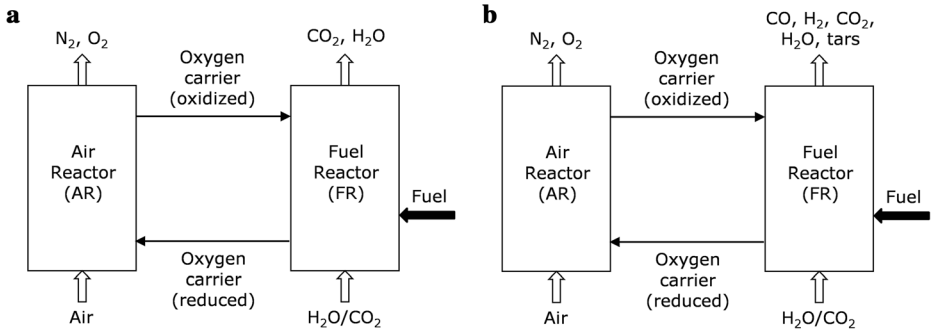

Fig. 1 Schematic illustrations of **a** chemical-looping combustion (CLC) and **b** chemical-looping gasification (CLG)

about chemical-looping, as well as an overview of trends and developments, can be found elsewhere (Lyngfelt et al. 2001; Adánez et al. 2012).

Suitable process temperatures vary slightly for different oxygen-carrier materials but are usually considered to be within the range of 850–1050 °C. The most commonly proposed way to design a chemical-looping combustor is to use circulating fluidized-beds (CFBs) with oxygen-carrier particles as bed material instead of an inert bed material as used in conventional applications.

In regular chemical-looping combustion, gaseous fuel is assumed to react with the solid oxygen carrier. However, some oxygen-carrier materials can release gaseous oxygen, which was found to enhance fuel conversion. This process is referred to as chemical looping with oxygen uncoupling (CLOU) (Imtiaz et al. 2013).

The first chemical-looping combustion pilot, based on interconnected fluidized-bed technology, was constructed and commissioned in 2003. Today, chemical-looping operation in the literature involves at least 9000 h in 34 pilot units (Lyngfelt et al. 2018). Most of the operational experience with chemical-looping combustors has been obtained using gaseous fuels and manufactured oxygen carriers. In the case of chemical-looping combustion with solid fuels, however, more often low-cost materials based on minerals or waste materials are used. There are two main reasons for the focus on such low-cost materials. Firstly, solid fuels usually contain significant quantities of ash, which is expected to decrease the lifetime of the oxygen carrier. Secondly, the requirements with respect to reactivity of an oxygen carrier material for solid fuels tend to be lower as compared to hydrocarbon-based, gaseous fuels. This is due to the higher chemical stability of, for example, methane in natural gas in contrast to the more reactive gases carbon monoxide (CO) and hydrogen (H_2), which are intermediate products in solid fuel conversion.

Chemical-looping gasification (CLG) is built around the same principles as indirect fluidized bed gasification, with two interconnected fluidized beds—air reactor and fuel reactor/gasifier—but uses an oxygen carrier instead of sand as bed material. This has potential advantages as compared to normal indirect gasification. Firstly, a more oxidizing environment and the presence of oxygen carriers in the gasifier reduces the tar content (Lind et al. 2013; Berdugo Vilches et al. 2017). Secondly, the cost of gas cleaning is reduced, as essentially all the fuel is converted in the fuel reactor, and none in the air reactor, thus reducing the volume of gas needing clean-up. Moreover, as no CO_2 is expected from the air reactor the CO_2 stream is concentrated with the syngas and, hence, amiable for capture. If biomass is used as fuel and capture of the CO_2 is applied, negative emissions of CO_2 can be achieved, while at the same time producing valuable syngas that can be used for, for example, biofuel production.

In this work, the processes chemical-looping combustion and chemical-looping gasification are demonstrated using a by-product from the steel industry as oxygen carrier material.

1.2 Potential technology impact

For chemical-looping gasification, there are presently no techno-economic assessments available, so only chemical-looping combustion will be addressed below.

As said, the process can ideally accomplish CO_2 capture without any gas separation step. Gas separation is normally the major part of the cost of carbon capture and storage, which suggests a potential for chemical-looping combustion to achieve dramatic cost reductions. A techno-economic analysis of chemical-looping combustion using solid fuel, (Lyngfelt and Leckner 2015) indicated the following:

- Chemical-looping combustion technology, although based on a fundamentally different principle, has very large similarities with commonly used combustion in circulating fluidized bed boilers. The added cost of chemical-looping combustion facility as compared to a circulating fluidized bed boiler could be very low, e.g., < 1 €/ton CO_2 captured.
- The major cost appears to be the CO_2 compression. The compression of the CO_2 captured to the pressure needed for transportation and injection is inevitable for all CO_2 capture and storage technologies. For established CO_2 capture technologies, the cost of capture is significantly higher than the cost of compression.
- The actual capture cost of chemical-looping combustion has two major, interrelated components, the downstream treatment of the concentrated CO_2 stream coming from the fuel reactor and the oxygen carrier.
- The downstream treatment cost will depend on the purity of the CO_2 attained, which results from the performance of the fuel reactor, i.e., how well the fuel added is converted to the desired end products CO_2 and H_2O, cf. Fig. 1a. The solution to inadequate conversion is to burn any unconverted combustibles by the addition of oxygen, also called oxy-polishing. This comes with a cost and energy penalty for gas separation, i.e., oxygen production, just like in CO_2 capture with oxy-fuel combustion. Normally, the performance of the fuel reactor is quantified as the oxygen demand, i.e., the fraction of total oxygen needed that would need to be supplied to achieve full conversion in the oxy-polishing step. So, if the oxygen demand is for instance 10%, the need for oxygen would be 10% of what would be needed for oxyfuel combustion if it were used instead of chemical-looping combustion. In other words, the need for gas separation would then be reduced by a factor of ten, as compared to oxyfuel combustion. This is an example, pilot operation of chemical-looping shows oxygen demands ranging between 0 and 30% depending on fuel, oxygen carrier, reactor design, and other operational conditions.
- The cost of oxygen carrier is a function of the price of the oxygen carrier and its lifetime. For solid fuels, expensive manufactured oxygen carriers are normally not considered, and the focus is more on natural ores—like manganese, iron, or ilmenite—being mined and readily available. Estimations of the cost of oxygen carrier using such materials are around a few Euros per ton of CO_2 captured. However, there are uncertainties both in the estimation of lifetime and the actual price of the material, including pre-processing to adequate particle size. Therefore, the possibility to use waste materials instead involves a potential for further cost reduction, as well as a way of assuring that estimated low costs of oxygen carrier are not compromised by shorter lifetimes than expected.
- Several studies indicate low costs of CO_2 capture with chemical-looping combustion for using coal, i.e., 16–26 €/ton of CO_2 (Lyngfelt and Leckner 2015), 26 €/ton (European Technology Platform for Zero Emission Fossil Fuel Power Plants 2011), and 32 €/ton (Haaf et al. 2018). The latter found a lower cost for biomass, 24 €/ton. Thus, there is a potential for cutting the cost of CO_2 capture by at least a factor of two compared to established technologies.

In addition to low-cost efficient CO_2 capture, there are other potential advantages with using biomass in chemical-looping combustion:

- Reduced costs and reduced operational difficulties from fouling/corrosion caused by aggressive ash components such as potassium (K). This is a major issue in combustion of biomass.

- The possibility of increasing steam data, i.e., efficiency of power generation. The difficulties with fouling/corrosion lead to the design of biomass boilers with lower steam temperatures.
- Extended range of fuels which can be used, e.g., fuels with higher content of K. For instance, straw-based biomass, which typically has a potassium content much higher than woody biomass, could become more viable for use in combustion for energy production and negative emissions.
- Reduced or eliminated emissions of nitric oxide (NO).

The first three of these opportunities are illustrated by Fig. 2. The explanation for the fourth is that no NO forms in the air reactor, i.e., at least as long as no nitrogen-containing fuel leaks from the fuel reactor. Thus, the stream of gas from the air reactor could be very clean, whereas undesired nitrogen compounds formed in the fuel reactor can be removed from the CO_2 stream and prevented from escaping to the atmosphere.

The assessments of the need for future negative emissions are on a scale of many Gt of CO_2 yearly and the potential impact of chemical-looping combustion on the CO_2 capture cost is large. Thus, this technology potentially could lead to enormous cost savings.

Although chemical-looping has been well studied in smaller pilots, there are no experiences on the commercial scale and there seems to be no real industrial involvement in any demonstration projects. This is explained by the fact that there is still a very low, if no, price on CO_2 emissions from fossil fuels, and for negative emissions of CO_2 with biomass, there is no recompense. Nevertheless, a few large-scale CO_2 capture and storage projects, with one exception on fossil fuels, have been realized and are in operation. But with no real market for CO_2 capture, no industry will take the costs and risks of bringing the technology to the commercial scale.

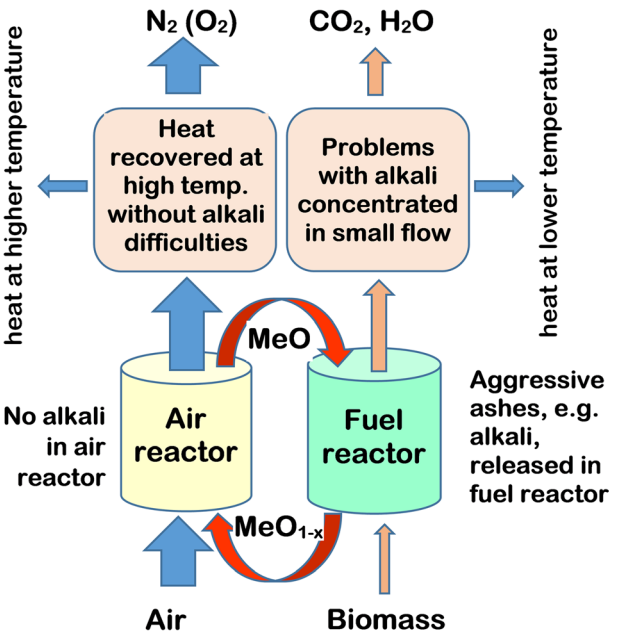

Fig. 2 Potential advantages of using biomass in chemical-looping combustion with respect to ash components

2 Experimental

2.1 Chemical-looping test units

2.1.1 300 W unit

The laboratory-scale continuous 300 W unit requires approximately 250–400 g of oxygen-carrier particles, depending on their density. The reactor is 300 mm high and has two reactor chambers: an air reactor and a fuel reactor. The fuel reactor has a cross-section of 25 mm × 25 mm, whereas the base of the air reactor is 25 mm × 42 mm and contracts to 25 mm × 25 mm in the riser section. Figure 3 shows the working principle of the reactor unit: high gas velocities cause the particles to leave the air reactor and enter the gas-solid separator placed on top flange of reactor unit (not shown in the figure). The particles fall back and enter the inlet of the J-type loop seal. This causes particles at the outlet of the loop seal to drop down onto the bubbling bed of the fuel reactor (through the return orifice). From the bottom of the fuel reactor, the particles flow back into the air reactor via the lower loop-seal. The air reactor is fluidized with air, the loop seals are fluidized with argon (Ar) and the fuel reactor is fluidized with methane (CH_4) during fuel operation or argon for determination of CLOU behavior.

The off-gases from the reactors are separately cooled to 4 °C and filtered. The fuel-reactor flue gas passes a water seal, which generates a slight overpressure in the fuel reactor and reduces leakage of air into the fuel reactor. The dried gases are analyzed for CO, CO_2, and CH_4 using infrared (IR) sensors and oxygen (O_2) using paramagnetic sensor. The fuel-reactor flue gas is also analyzed in a gas chromatograph (GC) to verify these gas species and to further quantify nitrogen (N_2) and H_2.

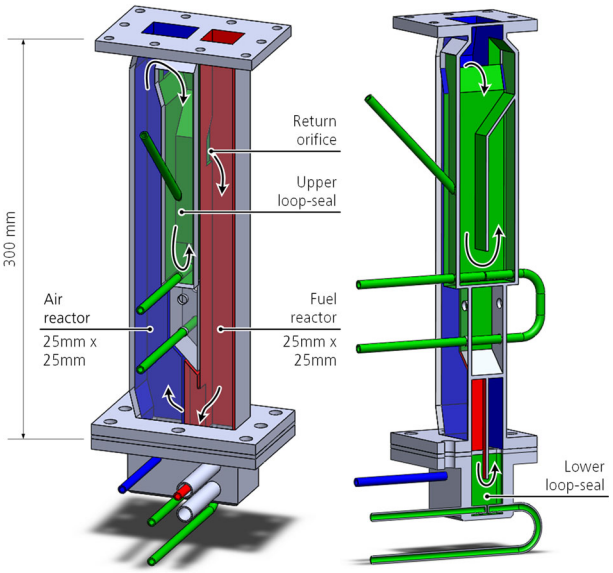

Fig. 3 Illustration of the 300 W chemical-looping combustion reactor

2.1.2 10 kW unit

The 10 kW CLC unit consists of a fuel reactor, an air reactor, a riser, a cyclone, and loop seals. In the fuel reactor, the fuel is gasified by steam, whereupon gasification products are oxidized by the oxygen carrier, which, in turn, is reduced. The fuel reactor is also equipped with a recirculation loop, which is not shown in Fig. 4, the function of which is to return elutriated char particles to the fuel reactor. In the air reactor, the oxygen carrier is oxidized. In the riser, the oxygen carrier particles are lifted and circulated back to the fuel reactor via the cyclone—a gas–solids separator—and the upper loop-seal. The upper and lower loop seals inhibit gas leakages between air reactor and fuel reactor.

The fuel reactor is fluidized with steam and operated as a bubbling bed. The fuel is introduced 100 mm into the bed and the total bed height, i.e., the distance from the gas distribution plate to the overflow exit is 273 mm. The fuel reactor has an internal

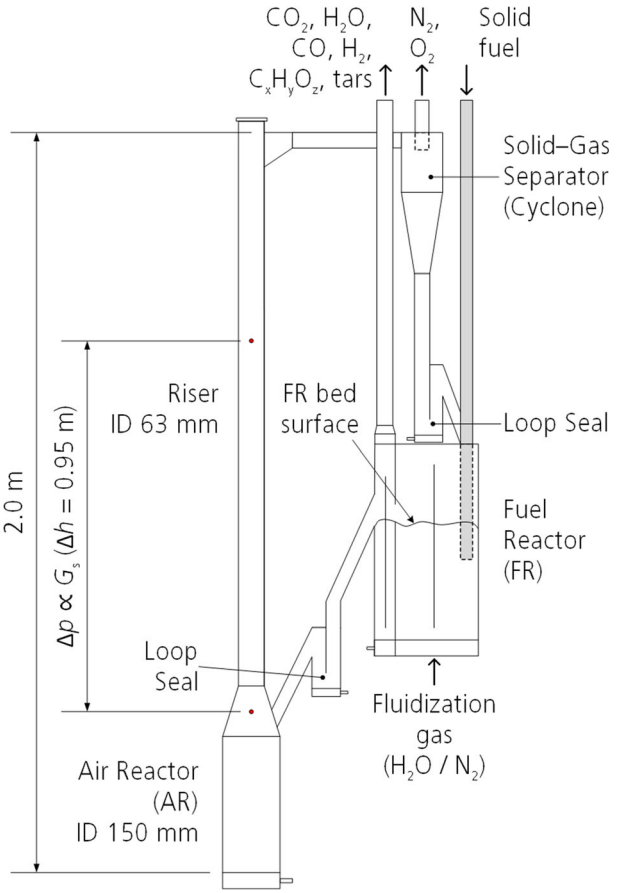

Fig. 4 Schematic of the 10 kW chemical-looping reactor. The measured pressure difference along the riser section, which is assumed to be proportional to the solids circulation, G_s, is shown. The recirculation loop connected to the fuel reactor is not shown

partitioning to prevent surface by-pass and, consequently, give the particles a more even residence-time distribution. The total solids inventory is around 15 kg, out of which approximately 5 kg is in the fuel reactor. A schematic of the unit is shown in Fig. 4. A more detailed description of the 10 kW unit can be found elsewhere (Linderholm et al. 2012).

The reactor is placed in an electrically heated furnace, which is necessary to reach the desired operating temperatures at start-up. Due to heat losses from the system, heat also needs to be supplied to the reactor system during normal operation with fuel.

After passive cooling in finned pipes, the air reactor flue gas passes through a textile filter, where elutriated particles are trapped. The fuel-reactor flue gas is led through a water seal, which generates a slight overpressure in the fuel reactor with the purpose to control the pressure balance of the reactor system.

Cleaned and dried gas samples from both chimneys are led to gas analyzers, where the fractions of O_2 and CO_2 are determined in the flue gas of the air reactor, and, respectively, the fractions of CO_2, CO, CH_4, O_2, and H_2 in the flue gas of the fuel reactor. The instruments used are Rosemount NGA2000 and Sick Sidor. CO_2, CO, and CH_4 are measured by IR sensors, O_2 with a paramagnetic sensor and H_2 with a thermal conductivity sensor. Bronkhorst mass flow controllers regulate all incoming gas flows and pressure transducers are used to monitor differential pressures related to bed heights and particle flows. Temperature in the system is monitored by three K-type thermocouples that are in the air reactor, in the cyclone, and in the fuel reactor.

2.2 Oxygen carrier material

Important criteria for oxygen carriers used in chemical looping with solid fuels include:

- High reactivity with fuel and oxygen and ability to convert the fuel fully to carbon dioxide (CO_2) and water (H_2O)
- Physical integrity during long periods of operation
- Low cost
- Preferably being environmentally sound

Combustion of solid fuels inevitably involves the release of fuel ash, which means that a large mass flow of ash must be discharged continuously. This ash discharge, and possibly also fouling by ash, is expected to limit the lifetime of the oxygen carrier. Consequently, oxygen carriers of low cost are the primary choice for chemical-looping combustion and chemical-looping gasification with solid fuels. Natural minerals are such a low-cost option for oxygen carriers, industrial by-products like slag the from Linz–Donawitz (LD) process are another option. The feasibility of using minerals as oxygen carriers in chemical-looping combustion has previously been investigated and demonstrated (Linderholm et al. 2012; Moldenhauer et al. 2018a; Schmitz et al. 2016; Linderholm et al. 2017).

LD slag is the second largest by-product in steelmaking. It is formed by reactions of slag formers (e.g., burned lime), silica, iron, and other components during conversion of carbon-rich molten pig iron into steel in the basic oxygen-blown converter process (aka Linz–Donawitz process). A typical steel mill may generate 100–300 kton/year, of which less than half can be recirculated internally to the blast furnace. There is very limited demand for LD slag for other purposes.

The chemical composition of LD slag makes it interesting as oxygen carrier. Table 1 shows recent analyses from our source of two samples of LD slag: one sample as received and the other one after heat treatment at 950 °C in air for 24 h. LD slag consists mostly of calcium (Ca), iron (Fe), magnesium (Mg), silicon (Si), manganese (Mn), and vanadium (V) but contains several more trace elements.

It shall be noted that combined Fe–Mn–Si oxides are among the more interesting combined oxide systems for oxygen-carrying purposes (Rydén et al. 2014a; Källén et al. 2015). LD slag has previously been examined as oxygen carriers in experiments involving combustion (Wang et al. 2017) and tar reforming (Keller et al. 2014).

LD slag is generated after the molten steel have been tapped off from the converted vessel. The remaining molten slag is then poured into a slag pot which, subsequently, is discharged outside. LD slag is formed during cooling and solidification of the melt. The resulting slag is rather homogenous and possibly of more predictable quality than virgin minerals. It has a high skeletal density (3500 kg/m^3) but its bulk density (1200–1400 kg/m^3) is similar to that of sand.

The LD slag used for these experiments was produced by SSAB Merox AB. A sample of 180 t was taken from a storage pile containing about 1 million tons. The sample was dried, crushed, and sieved in a sieve shaker using two sieves (400 μm and 100/150 μm). The result was 38 t of particulate LD slag in the size range 100–400 μm to be used in several research activities.

2.3 Fuels used

For the tests conducted in the 300 W unit, the fuels used were syngas, i.e., 50 vol% H_2 in CO and methane.

Table 1 Composition of LD slag samples before fuel operation determined with inductive coupled plasma sector field mass spectrometry (ICP-SFMS) according to SS-EN ISO 17294-1,2 (mod) and EPA method 200.8 (mod). The balance of "total element + LOI" consists mainly of oxygen

	As received		Heat treated (950 °C in air)	
	(Mass%)	(Atom%)†	(Mass%)	(Atom%)†
Dry matter	97.8	–	100	–
LOI*	7.0	–	0.9	–
Elemental composition				
Ca	27.3	46.5	29.7	47.5
Fe	13.7	16.7	13.9	15.9
Mg	6.0	17.1	6.3	16.7
Si	4.8	11.6	5.1	11.7
Mn	2.2	2.7	2.4	2.8
V	1.6	2.1	1.6	2.0
Ti	0.7	1.0	0.7	1.0
Al	0.5	1.3	0.5	1.3
Cr	0.3	0.4	0.4	0.4
P	0.2	0.4	0.2	0.4
S	0.1	0.2	0.1	0.2
Total element	64.4	100	61.8	100

*Loss on ignition, i.e., weight loss upon heating to 1000 °C in air and consecutive cooling

† Without oxygen

The fuels used for chemical-looping combustion and chemical-looping gasification in the 10 kW unit are wood char, wood pellets, and steam-exploded wood pellets (aka black pellets). The wood char is produced by heat treatment (≈ 450 °C for > 10 h) in inert atmosphere. The steam-exploded wood pellets are intended for co-firing with coal and produced by exposing woody biomass to pressurized steam followed by a sudden pressure release and pelletization.

A major difference between the fuel Swedish wood char and the two other fuels used is the volatile content. Volatiles are released quickly upon heating of the particles and fuels rich in volatiles can create gas bubbles, which pass through the bed too quickly to be fully converted. The volatile content of the different fuels used, as well as other properties, are shown in Table 2.

The size of the fuel particles affects both the reactivity and fluid-dynamic properties of the particles. Small particles devolatilize faster due to a higher surface-to-volume ratio. On the other hand, small particles tend to follow the gas stream, whereas larger particles are likely to remain in the bed for longer periods of time. Hence, use of small fuel particles decreases fuel residence time in the bed, which can lead to lower solid-fuel conversion. A carbon stripper can be used to separate fuel and oxygen-carrier particles if there is a sufficient difference in terminal velocity between the two types of particles.

2.4 Definitions and data evaluation

2.4.1 300 W unit

The ability of an oxygen carrier to convert fuel to CO_2 is expressed by the CO_2 yield γ_{CO2}, see Eq. (1), where $[i]_{FR}$ are the volume fractions of species i measured in the fuel reactor. The calculation is based on a carbon balance over the fuel reactor outlet.

Table 2 Properties of the solid fuels used for investigations in the 10 kW unit

	Swedish wood char	Wood pellets	Steam-exploded wood pellets
Alternate notation	Wood char	Crushed wood pellets, sawdust	Black pellets, heat-treated stem wood
Producer	Skogens Kol	n/a	Arbaflame
Lower heating value (MJ/kg, as received)	29.8	17.7	18.6
Size, d_{50} (mm, as received)	0.8	0.6	1.6
Proximate analysis (mass%, as received)			
Fixed carbon	73.9	15.1	18.7
Volatiles	16.7	78.4	74.2
Moisture	3.9	6.0	6.9
Ash	5.5	0.5	0.3
Ultimate analysis (mass%, dry and ash free)			
C	86.9	50.9	53.5
H	3.2	6.0	6.0
O	9.5	43.0	40.3
N	0.4	0.1	0.1
S	0.03	0	0
Chemical-looping operation investigated	CLC	CLC, CLG	CLC, CLG
Total amount of fuel added (g)	2430	850	14,760
Fuel operation time (h)	5.1	21.6	1.2

$$\gamma_{CO2} = \frac{[CO_2]_{FR}}{[CO_2]_{FR} + [CO]_{FR} + [CH_4]_{FR}} \quad (1)$$

2.4.2 10 kW unit

Solids circulation One way to quantify the circulation of solids in a circulating fluidized bed (CFB) reactor is through the mass flux of solids, G_s, which expresses the circulation as mass flow per area in kg/m²s. Normally, the cross-sectional area of the riser is used as reference. This allows for comparison of solid circulation of CFB units of different sizes. It is usually not possible to measure the mass flux of solids directly, which is why it is calculated based on pressure measurements, which are extrapolated in order to obtain the bed density at the exit of the riser (Johnsson et al. 1999). For practical reasons, this estimation is further simplified and adapted to the 10 kW unit, see Eq. (2). CI is referred to as circulation index and is based on a pressure measurement over the riser, i.e., Δp and Δh, cf. Fig. 4, on the superficial gas velocity, u_0, and on the terminal velocity, u_t, which is approximated according to Kunii and Levenspiel (Kunii and Levenspiel 1991). The g in Eq. (2) is the gravimetric constant. Hence, the circulation index, CI, represents the gross amount of particles in the chosen riser segment, i.e., the sum of particles traveling upwards and downwards and gives an overestimation of the true mass flux of solids. The circulation index is assumed to be proportional to the real mass flux.

$$\mathrm{CI} = -\frac{1}{g} \cdot \frac{\Delta p}{\Delta h} \cdot (u_0 - u_t) \quad (2)$$

Fuel conversion Fuel that enters the fuel reactor can follow one of three routes:

1. Conversion to gas in the fuel reactor, which is the desired case.
2. Conversion in the air reactor. Some char will inevitably follow the flow of oxygen carrier to the air reactor, where it is oxidized to CO_2. This is expressed by Eq. (3).
3. Exit the fuel reactor via the chimney as unconverted char (not monitored).

Gaseous species produced in the fuel reactor are either volatile fuel-compounds or products of char gasification. Volatiles include mainly CH_4, H_2, CO, and CO_2. Higher hydrocarbons are also present to smaller extent, but these are only measured up to propane (C_3H_8).

The degree of fuel oxidation, η_{fuel}, is the ratio of the amount of oxygen consumed by the oxygen carrier in the air reactor, $\dot{n}_{O2,OC,AR}$, and the stoichiometric amount of oxygen needed for full conversion of fuel to CO_2 and H_2O, $\dot{n}_{O2,stoich}$. In Eq. (3), the oxygen uptake in the air reactor, $\dot{n}_{O2,OC,AR}$, is calculated by subtracting the outgoing molar flow of O_2, $\dot{n}_{O2,AR,out}$ and the outgoing molar flow of CO_2, $\dot{n}_{CO2,AR,out}$ from the ingoing molar flow of O_2, $\dot{n}_{O2,AR,in}$.

$$\eta_{fuel} = \frac{\dot{n}_{O2,OC,AR}}{\dot{n}_{O2,stoich}} = \frac{\dot{n}_{O2,AR,in} - \dot{n}_{O2,AR,out} - \dot{n}_{CO2,AR,out}}{\dot{n}_{O2,stoich}} \quad (3)$$

Based on molar flow of CO_2 leaving the air reactor, $\dot{n}_{CO2,AR,out}$ and the molar flow of carbon supplied with the fuel, $\dot{n}_{C,fuel}$, the fraction of fuel carbon that leaks into the air reactor, $f_{C,AR}$, is determined, see Eq. (4). The flow of CO_2 leaving the air reactor is

compensated for the atmospheric concentration of CO_2, which was approximately 400 ppm during the time of the experiments. Closely connected to this carbon leakage is the carbon capture efficiency, η_{CC}, which reflects unconverted char reaching the air reactor and being oxidized to CO_2, see Eq. (5). The carbon capture efficiency is the ratio of the carbon that leaves the fuel reactor via the chimney, i.e., converted to gas or as char, to the total flow of carbon into the reactor system.

$$f_{C,AR} = \frac{\dot{n}_{CO2,AR,out}}{\dot{n}_{C,fuel}} \tag{4}$$

$$\eta_{cc} = 1 - f_{C,AR} \tag{5}$$

Another way to evaluate the conversion of fuel, which gives more detailed information about the different steps of conversion and selectivity, is to quantify the different species in the exhaust gas of the fuel reactor. The measurement equipment used, cf. Section 2.1.2, allows for monitoring of hydrocarbons up to C_3H_8. The different carbon species are distinguished and calculated according to Eqs. (6)–(10), where f_i is the fraction of species i, and $\dot{n}_{i,FR}$ is the molar flow of species i in the flue gas of the fuel reactor. A special denotation was chosen for the fraction of CO_2, i.e., γ_{CO2}, to highlight that this is the desired carbon fraction.

$$\gamma_{CO2} = \frac{\dot{n}_{CO2,FR}}{\dot{n}_{CO2,FR} + \dot{n}_{CO,FR} + \sum_x \left(x \cdot \dot{n}_{CxHy,FR}\right)} \tag{6}$$

$$f_{CO} = \frac{\dot{n}_{CO,FR}}{\dot{n}_{CO2,FR} + \dot{n}_{CO,FR} + \sum_x \left(x \cdot \dot{n}_{CxHy,FR}\right)} \tag{7}$$

$$f_{CH4} = \frac{\dot{n}_{CH4,FR}}{\dot{n}_{CO2,FR} + \dot{n}_{CO,FR} + \sum_x \left(x \cdot \dot{n}_{CxHy,FR}\right)} \tag{8}$$

$$f_{C2} = \frac{\dot{n}_{C2Hy,FR}}{\dot{n}_{CO2,FR} + \dot{n}_{CO,FR} + \sum_x \left(x \cdot \dot{n}_{CxHy,FR}\right)} \tag{9}$$

$$f_{C3} = \frac{\dot{n}_{C3Hy,FR}}{\dot{n}_{CO2,FR} + \dot{n}_{CO,FR} + \sum_x \left(x \cdot \dot{n}_{CxHy,FR}\right)} \tag{10}$$

The air-to-fuel ratio, AFR, is the molar ratio of oxygen in the air fed to the air reactor, $\dot{n}_{O2,AR,in}$, and the stoichiometric amount of oxygen needed for complete combustion of fuel, $\dot{n}_{O2,stoich}$, see Eq. (11). A high air-to-fuel ratio also indicates a high circulation. The air-to-fuel ratios used in the 10 kW pilot unit are much higher than what would be feasible in a large-scale process. The reason for this is that the 10 kW unit was designed for flexibility with respect to, e.g., oxygen carrier, fuel type, and fuel input. The air flow in the

riser is used to vary solids circulation and when high rates of solids circulation are tested together with a low fuel input, the air-to-fuel ratio reaches very high values. It was used for the evaluation of the results because it expresses both fuel flow and solids circulation in one value.

$$\mathrm{AFR} = \frac{\dot{n}_{\mathrm{O2,AR,in}}}{\dot{n}_{\mathrm{O2,stoich}}} \tag{11}$$

3 Results

3.1 Experiments in 300 W unit

3.1.1 CLOU properties

The CLOU effect, i.e., the ability to release of gaseous oxygen of LD slag was determined at the beginning of the campaign and at its end, see Fig. 5. This was done by monitoring the oxygen released in the fuel reactor, which was fluidized with argon. The fresh material showed little CLOU effect, but the concentration of released oxygen was always higher than the concentration of oxygen due to leakage, i.e., 24%, 49%, and 96% (average based on 3–4 measurements) at 840 °C, 890 °C, and 940 °C, respectively. The used material showed a more distinct CLOU effect and the released oxygen was usually about three times higher than oxygen due to leakage. The amount of oxygen released by the used material increased with increasing temperature and varied between 1.1 and 1.7 vol% between 850 and 950 °C at a flow of 1 L_n/min of argon. It appears as if CLOU properties developed during the first day of fuel operation, i.e., 2.7 h of operation with syngas, which corresponds to about 85 redox cycles.

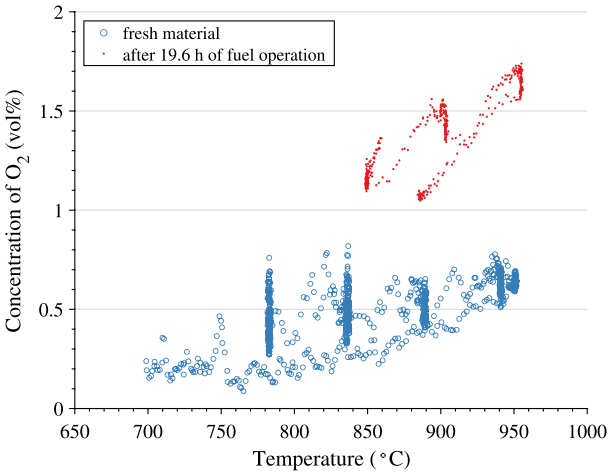

Fig. 5 Oxygen release of LD slag oxygen carrier in inert atmosphere (1 L_n/min of argon) at varied temperature. The concentration of O_2 at the outlet of the air reactor was 18.2–18.5 vol% with the fresh material and 19.3–19.5 vol% with the material after fuel operation. Each data point represents a 10 s average

3.1.2 Fuel conversion

With syngas as fuel, a very high CO_2 yield, up to 99.9 mol%, was achieved at 900 °C and a specific fuel-reactor bed mass of 280–340 kg/MW_{th}, see Fig. 6a. Initially, however, fuel conversion at similar conditions was lower, i.e., 98.1–98.7 mol% at 270–365 kg/MW_{th}. This initial phase with lower fuel conversion lasted approximately a little more than 2 h. It seems likely that this improvement in fuel conversion is correlated to the development of CLOU properties described in Section 3.1.1. Syngas conversion with the LD slag-based oxygen carrier is higher than that of all but one manganese ore-based oxygen carriers tested in this unit; five materials published (Moldenhauer et al. 2018a, b), as well as four materials unpublished.

Syngas conversion improved toward higher temperatures and higher specific fuel-reactor bed masses. Initially, experiments in the 300 W unit with LD slag as oxygen carrier were conducted with syngas as fuel at 900 °C. The order, in which the different settings were recorded, is indicated by the numbers next to the data points in Fig. 6a, whereas data points 1–6 correspond to the first 3 h of fuel operation, and data point 7 was recorded after methane was used as fuel, i.e., after about 17 h of fuel operation. Hence, the high degree of variation seen in the data points representing 900 °C is believed to be a result of an activation of the material.

After fuel testing with syngas, a series of experiments was performed with methane as fuel, see Fig. 6b. Fuel conversion varied clearly with temperature as well as with specific fuel-reactor bed mass; between 250 and 350 kg/MW_{th}, and 900 and 950 °C, CO_2 yields between 46 and 60 mol% were achieved. This is somewhat higher than fuel conversion achieved with most manganese ore-based oxygen carriers that were tested in this unit; four materials published (Moldenhauer et al. 2018a, b), as well as four materials unpublished.

3.1.3 Particle analysis

Particle attrition was monitored during fuel operation in the 300 W unit, and, additionally, attrition behavior of fresh and used particles was analyzed in a customized jet-cup attrition rig (Rydén et al. 2014b). The different attrition rates as well as fuel operation time, bulk density,

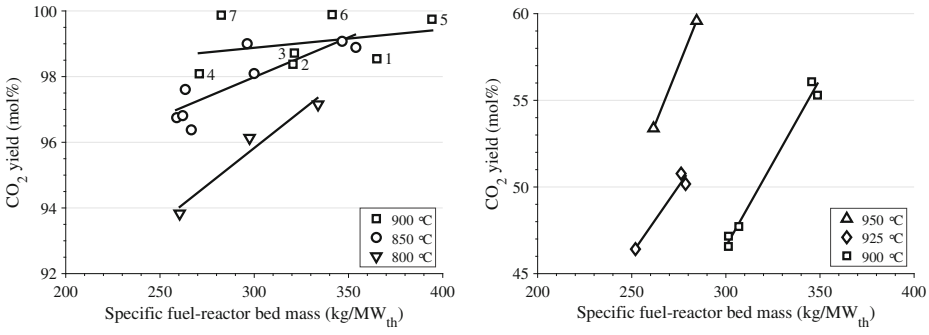

Fig. 6 Fuel conversion, i.e., CO_2 yield γ_{CO2}, as a function of the specific fuel-reactor bed mass at different temperatures with **a** syngas and **b** methane as fuel. The numbers next to the data points in subfigure **a** indicate the order of the experiments at 900 °C; data points 1–6 were carried out consecutively within the first 3 h of fuel operation, and data point 7 was carried out after 17 h of fuel operation

and particle size distribution are presented in Table 3. The bulk density decreased significantly despite a widening of the particle size distribution. This suggests that the particle density decreased more than the bulk density did.

Light microscope images of fresh and used LD slag particles were produced, see Fig. 7. The images show that there is a clear difference between the fresh and used samples and that the particles of each sample are heterogeneous. This indicates that the material contains various phases, which are transformed from fresh state to used state. The sample of used particles appears to be somewhat less heterogeneous than the fresh sample.

X-ray powder diffractometry (XRD) was conducted to analyze the crystal structure of different samples of LD slag: (1) a fresh sample "as received," i.e., not heat-treated, (2) an oxidized sample extracted from the air reactor after 20 h of fuel operation, and (3) a reduced sample extracted from the fuel reactor after 20 h of fuel operation. The samples were analyzed in the interval $2\theta = 15\ldots75°$ with 0.05° steps. The instrument used was a Bruker D8 Advance with a thin-film detector and CuKα1/2 radiation at 45 kV and 40 mA. The resulting diffractograms yield complex phase chemistry and many peaks allow diverse interpretations. The main crystalline phases identified in the three samples analyzed are presented in Table 4. The fresh sample "as received" contains few major phases and many minor phases, whereas the two used samples contain more major phases than minor phases. The general impression, which is supported by the light microscope images, see Fig. 7, is that the used samples are somewhat more homogenous than the fresh sample. The fresh sample contains hydroxides and carbonates, which decompose upon heating in air, while reduced phases such as iron–magnesium oxide ((Fe,Mg)O) are oxidized. The sum of mass decrease due to decomposition and mass increase due to oxidation is negative and corresponds to a mass decrease, i.e., LOI, loss on ignition, of 7 mass%, see Table 1. Free magnesium oxide (MgO) was found in the used, oxidized sample, whereas the used, reduced sample contains calcium hydroxide ($Ca(OH)_2$), which was likely calcium oxide (CaO) in hot condition but was hydrated by air humidity after cooling. Based on the XRD analysis, the phases that are active during chemical-looping combustion are MgO, calcium–magnesium–vanadium oxide ($CaMgV_2O_7$), and calcium–silicon oxide (Ca_3SiO_5) in oxidized state and magnesium–titanium–iron–manganese–vanadium oxide ($(Mg,Ti,Fe,Mn,V)_3O_4$) and CaO in reduced state. Some of the other phases identified might be active during redox cycles, too. But as the XRD analysis performed was not quantitative no further conclusions can be drawn.

Table 3 Particle attrition, fuel operation time, poured bulk density, and particle size distribution

Fuel operation	(h)	
Syngas		14.1
Methane		5.9
Average attrition rate observed under redox conditions	(wt%/h)	0.58
Attrition index measured in a customized jet-cup attrition rig	(wt%/h)	
Fresh particles		0.97
Particles after 20 h of fuel operation		6.2
Bulk density determined based on standard ISO 3923-1	(kg/m^3)	
Fresh particles		1180
Particles after 20 h of fuel operation		1000
Particle sizes D_{10}, D_{50}, D_{90}	(μm)	
Fresh particles		148, 180, 235
Particles after 20 h of fuel operation		62, 167, 224

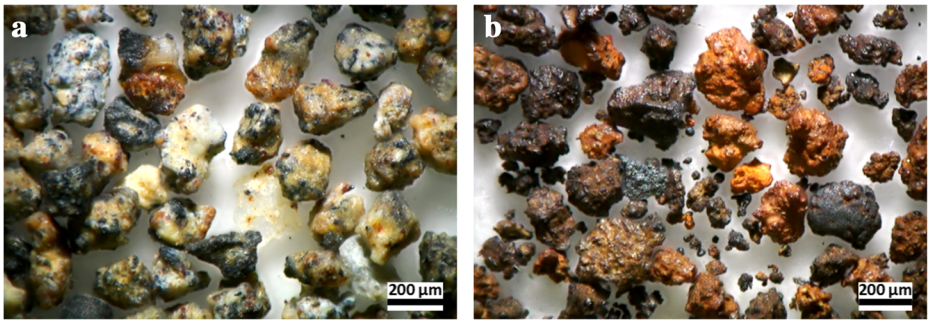

Fig. 7 Light microscope images of **a** fresh particles and **b** used particles

3.2 Experiments in 10 kW unit

3.2.1 Fuel conversion

Table 5 shows the experimental parameters that were investigated with LD slag as oxygen-carrier material.

A higher superficial gas velocity in the riser leads to a higher circulation index, see Fig. 8. The gas velocity in the riser was always higher than the average terminal velocity of the particles, i.e., 0.5–0.8 m/s. The relatively high variation of the circulation index for a given superficial gas velocity is likely a result of variations in the system inventory. In the gas–solids separator, a large amount of particles, not only fines, was elutriated from the system and, consequently, the system inventory varied between 12 and 17 kg, cf. Fig. 14.

The degree of fuel oxidation and carbon leakage to the air reactor at varied air-to-fuel ratio for the different fuels used are shown in Figs. 9 and 10. The degree of fuel oxidation increases with an increasing air-to-fuel ratio. With black pellets at very high air-to-fuel ratios, high degrees of fuel oxidation were achieved, i.e., 92 and 96%. In most cases, carbon leakage was below 1% of the fuel carbon and, except for a few outliers, all leakage was below 20%. Carbon leakage with wood char as fuel seems to be higher than with the other two fuels investigated. It should be noted that both the degree of fuel oxidation and carbon leakage to the air reactor

Table 4 Main crystalline phases identified by XRD in fresh and used samples of LD slag. Major phases that mark differences between the samples are displayed in italic characters

	Fresh, not heat-treated (as received)	Used, oxidized	Used, reduced
Major phases	*$Ca(OH)_2$, $CaCO_3$, (Fe,Mg)O*	$Ca_2Fe_2O_5$*, *MgO*, Ca_2SiO_4‡, *$CaMgV_2O_7$*, *Ca_3SiO_5*, $Ca_3Al_2O_6$	$Ca_2Fe_2O_5$*, *$(Mg,Ti,Fe,Mn,V)_3O_4$*, Ca_2SiO_4‡, *$Ca(OH)_2$*, $Ca_3Al_2O_6$
Minor phases	Ca_2SiO_4, $Ca_2Fe_2O_5$*, Ca_3SiO_5†, $(Fe,Ca)_2O_3$, $Ca_3Al_2O_6$, $CaMn_{14}SiO_{24}$, Ca_2SiO_4, $(Mg,Ti)_3O_4$, CaO	$CaFeO_2$, $(Fe,Mg)_2O_3$, $(Fe,Mg)_3O_4$	$(Al,Mg,Si,Fe)_7O_{10}$

*May contain Mg, Si, V, Mn, Al, and/or Ti

† May contain traces of Mg and/or Al

‡ May contain traces of Al and/or S

Table 5 Experimental parameters investigated in the 10 kW unit with LD slag as oxygen carrier for the different fuels used

		Black pellets	Wood char	Wood pellets
Superficial gas velocity in the riser	(m/s)	2.8–5.5	3.1–4.9	2.6–4.7
Air reactor temperature	(°C)	815–940	820–920	825–935
Fuel reactor temperature	(°C)	920, 965–980	965–985	980–985
Fuel flow	(g/min)	9.0–33.5	3.0–6.6	6.6–14.8
	(kW_{th})	2.8–10.4	1.5–3.3	1.9–4.4
Air-to-fuel ratio	(mol/mol)	1.0–8.1	3.0–7.9	2.9–7.0
Hydrogen-to-carbon ratio	(mol/mol)	4.7–13.0	5.8–22.7	10.0–22.4
Bed mass in fuel reactor	(kg)	5–6	5–6	5–6
Total bed mass	(kg)	12–17	12–16	12–14
Estimated specific fuel-reactor bed mass	(kg/MW_{th})	500–2100	4000–5300	1100–3200

contain rather high uncertainties that stem from the uncertainty when estimating the fuel flow, which is known to vary considerably at certain conditions. Therefore, the uncertainties for both the degree of fuel oxidation and carbon leakage to the air reactor are estimated to be up to 20% of the respective values.

The highest levels of carbon leakage that were measured here would be unfeasible for a large-scale carbon capture process. However, it is believed that the quantity of carbon leakage is reactor-specific and could be significantly lower for a large-scale system.

Figures 11 a–d show the different fractions of carbon species in the fuel reactor (γ_{CO2}, f_{CO}, f_{CH4}, and f_{C2}) at varied air-to-fuel ratio for the different fuels used. No C_3-species were detected during any of the experimental settings investigated. The highest CO_2 yield was achieved with wood char at a fuel input of 1.8 kW_{th}. Here, the CO_2 yield was 92% and the carbon leakage was low, i.e., 2.4%. Increasing the air-to-fuel ratio clearly improves fuel conversion, i.e., the CO_2 yield increases while the carbon fractions of C_2, CH_4, and CO decrease. When wood char was used as fuel, which has a low volatiles content, the CO_2 yield was generally somewhat higher than with black pellets or wood pellets, but this could also be an effect of the higher carbon leakage. Further, the amount of CH_4 was clearly lower than with black pellets or wood pellets and no C_2- or C_3-species were detected.

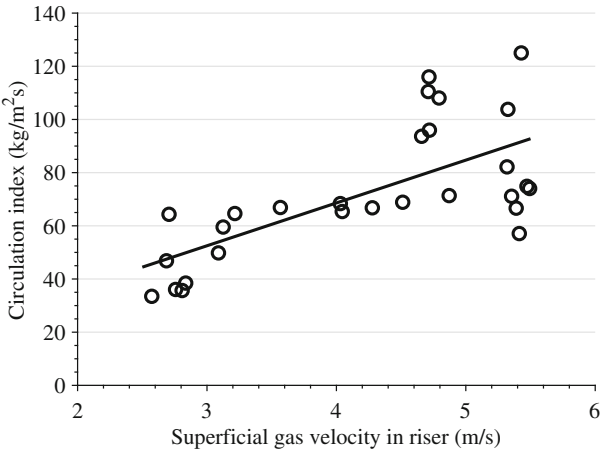

Fig. 8 Circulation index at varied superficial gas velocity in the riser

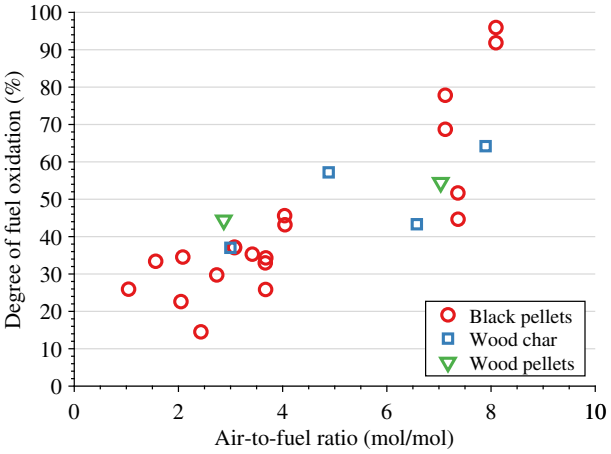

Fig. 9 Degree of fuel oxidation at varied air-to-fuel ratio, i.e., at varied air and fuel input. The degree of fuel oxidation does not include fuel oxidized in the air reactor. The fuel reactor temperature was 965–985 °C, except in one case with black pellets as fuel, at AFR = 3.4 when it was 920 °C. Values above 100% are not shown, i.e., one data point for wood pellets and two data points for wood char

Figure 12a shows the molar ratios of H_2/CO (Fig. 12) and of CO_2/CO (Fig. 12). The concentration of hydrogen measured was clearly above that of carbon monoxide, which can be attributed to the high hydrogen-to-carbon ratio in the fuel reactor, i.e., 4.7–22.4, due to the use of steam as fluidization agent. The concentration of H_2 measured was clearly below the equilibrium concentration calculated according to the water-gas shift reaction; measurements of H_2 were usually 10–40% lower than the equilibrium values, and in some cases, as much as 70% lower. The fraction of hydrogen measured in the fuel-reactor flue gas follows the same trend as the carbon fractions of CO (Fig. 11b). The highest average concentration of hydrogen was 36 vol% and was detected at 6.9 kW_{th} fuel input of black pellets, at an air-to-fuel ratio of 1.6 and a hydrogen-to-carbon ratio of 6.4. The lowest hydrogen fraction measured was

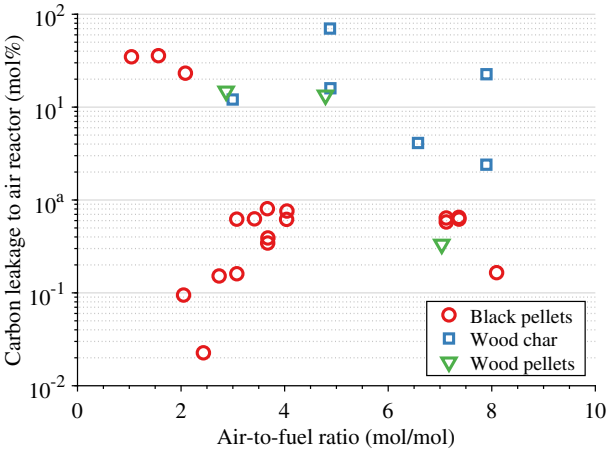

Fig. 10 Carbon leakage to the air reactor at varied air-to-fuel ratio. The fuel reactor temperature was 965–985 °C, except in one case with black pellets as fuel, at AFR = 3.4 when it was 920 °C. Negative numbers are not shown, i.e., one data point for black pellets

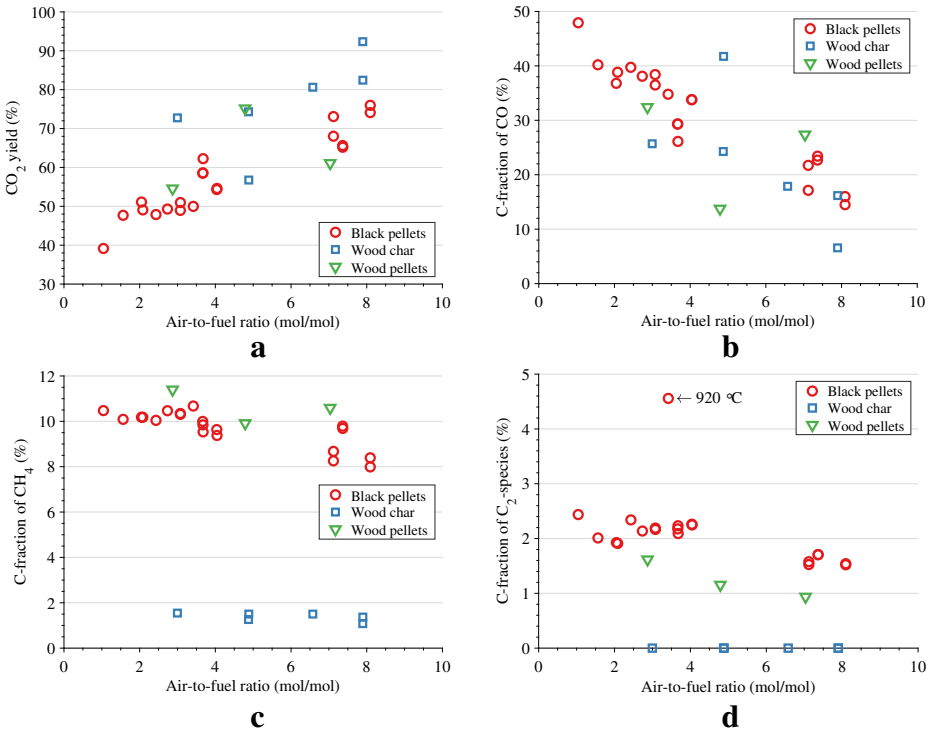

Fig. 11 Carbon fractions in the fuel reactor at varied air-to-fuel ratio for the different fuels used, **a** CO_2 yield, i.e., carbon fraction of CO_2, **b** carbon fraction of CO, **c** carbon fraction of CH_4, and **d** carbon fraction of C_2-species. No C_3-species were detected during any of the experimental settings investigated. The fuel reactor temperature was 965–985 °C, except in one case with black pellets as fuel at AFR = 3.4 when it was 920 °C

6.6 vol%. There is no clear correlation for fuel type or hydrogen-to-carbon ratio. The ratio of CO_2/CO increases linearly with the air-to-fuel ratio, see Fig. 12b, and thus follows the trends seen in Fig. 11.

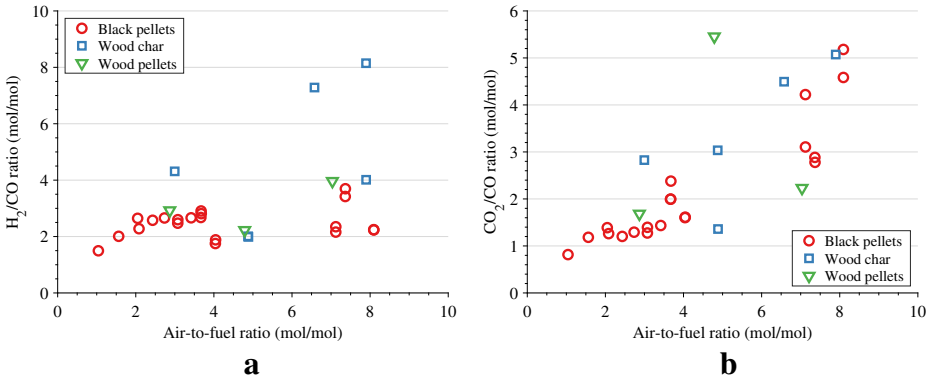

Fig. 12 Molar ratios of **a** H_2/CO and **b** CO_2/CO in the flue gas of the fuel reactor at varied air-to-fuel ratio, i.e., at varied air- and fuel input. The fuel reactor temperature was 965–985 °C, except in one case with black pellets as fuel at AFR = 3.4 when it was 920 °C

3.2.2 Particle attrition and lifetime

Initially, a large batch of LD slag-based oxygen carrier was prepared, ca. 30 kg, by removing particles larger than 500 μm followed by a washing process to remove fines, here defined as particles smaller than 63 μm. Thus, the amount of fines in the fresh material was reduced to about 5 wt%. During operation, material was elutriated from both air reactor and fuel reactor at a rather high rate. Elutriated material was collected in the bag filter connected to the air reactor cyclone, in a horizontal pipe section (between the fuel reactor outlet and the water seal) and in the water seal. After fines were quantified and removed from the elutriated material, the fraction larger than 63 μm, together with fresh material, was refilled into the system. Fines were not collected continuously, and the data was smoothed, i.e., interpolated.

The curve showing the cumulative amount of fines produced exhibits two jumps, at 4.3 h and at 8.9–9.4 h, see Fig. 13. There, larger amounts of fresh material were added to the system. The rate of fines production is low during the initial 4 h of fuel operation, as well as during the last 9 h of fuel operation. In between, fines are produced at a higher rate, see Fig. 14. Fresh oxygen carrier material, which contained about 5 wt% of fines, was added throughout the entire experimental campaign, see Fig. 13, though more fresh material was added initially. Hence, the change in fines production over time is likely a result of several factors.

1. Fresh oxygen carrier contains about 5 wt% of fines. Whenever fresh material is added these fines are assumed to be elutriated instantly.
2. Fresh LD slag was found to undergo changes during the first hours of fuel operation, cf. Sections 3.1.1 and 3.1.2. This transition is likely to cause stresses within the material that lead to increased attrition until the transition is complete.
3. Fines that are fuel ash can be neglected. A total of 22.8 h of the total fuel operation was conducted with fuels that contained little ash, i.e., 49 g in total and during 5.5 h wood char was used, which contained a total of 134 g ash.
4. Fines that are unconverted char were not quantified, but their influence on the fines production observed is assumed to be negligible. During the entire fuel operation time, the

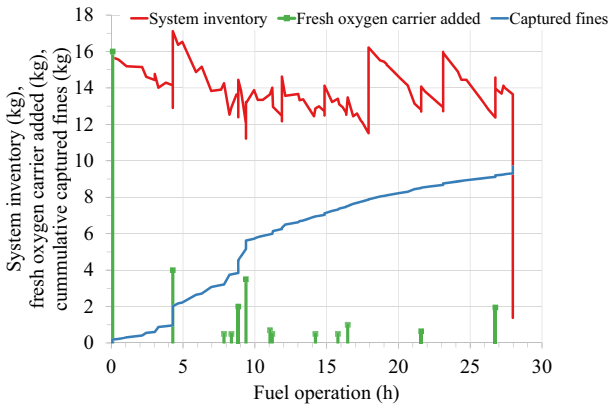

Fig. 13 System inventory, fresh oxygen carrier added, cumulative captured fines as a function of fuel operation time in the 10 kW unit. The refilling of used, sieved oxygen carrier is not shown separately but can be seen in the system inventory

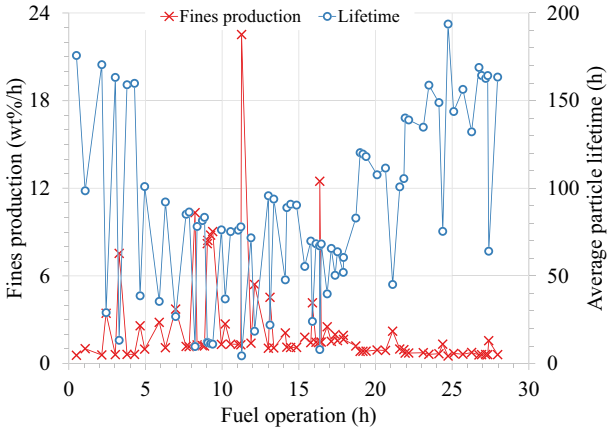

Fig. 14 Fines production rate and estimated average particle lifetime as a function of fuel operation time in the 10 kW unit

fuel added contained a total of fixed carbon of about 4.7 kg. If it is assumed that 5% of that carbon left the fuel reactor as char, this would correspond to a fraction of 2.5% of the total amount of fines produced.

It is assumed that the estimated average particle lifetime during the last part of the investigation, i.e., 110–170 h, is more representative for a large-scale operation. For a chemical-looping combustion boiler with a thermal power of 1000 MW, which contains a total of 850 t of solids inventory (500 t in the fuel reactor, 250 t in the air reactor, and the rest in gas–solids separators and loop-seals), the resulting regeneration rate of bed material would be in the range of 5–8 kg/MWh. It is emphasized that this number does not consider bed regeneration due to interaction with ash components, which may lead to sintering of the bed material. The typical regeneration rate of bed material used in conventional, biomass-fired CFB boilers is about 3 kg/MWh of quartz sand. If the interaction of an LD slag-based oxygen carrier with fuel ash is suitable and its cost is low, it can be a relevant oxygen-carrier material for large-scale chemical-looping combustion.

4 Summary, conclusions, and strategy recommendations

4.1 Summary and conclusions

LD slag is an industrial by-product that is produced in very large amounts, while its use is limited. Thus, the cost of an oxygen-carrier material for deployment in chemical looping applications, with respect to both raw material cost and cost of production, is potentially very low. LD slag was crushed, sieved, and heat treated before it was used for investigations in two small-scale chemical-looping reactor systems; (1) a unit with a nominal fuel input of 300 W_{th}, which was used with gaseous fuels syngas and methane for a total of 20 h with fuel operation and (2) a unit with a nominal fuel input of 10 kW_{th}, where investigations were conducted for a total of 28 h with three different biomass-based solid fuels.

In the 300 W unit, the material was activated during the first couple of hours with the addition of syngas. During activation, the material developed CLOU properties, i.e., the ability to release oxygen to the gas phase and the CO_2 yield increased notably. Very high degrees of syngas conversion were achieved, i.e., CO_2 yields of up to 99.9% at a specific fuel-reactor bed masses as low as 280 kg/MW_{th} and at a temperature of 900 °C. Methane conversion was far from complete, i.e., 60% at most at 280 kg/MW_{th} and 950 °C, but still high compared to manganese ore-based oxygen carriers tested in this unit.

During chemical-looping combustion in the 10 kW unit, CO_2 yields of 75–82% were achieved with all three fuels tested, while carbon leakage was very low in most cases, i.e., below 1%. In one case, when wood char was used as fuel, a CO_2 yield of 92% was reached, however, at a low fuel input, i.e., 1.8 kW_{th}. The carbon fraction of C_2-species in the fuel reactor was usually below 2.5% and no C_3-species were detected. The oxygen carrier lifetime was estimated to be about 110–170 h, without considering effects of interaction with ash components.

During part of the investigation in the 10 kW unit, the experimental parameters were adjusted to achieve chemical-looping gasification rather than chemical-looping combustion. For a gasification process, high fractions of H_2, CO, and possibly CH_4 are desirable, while carbon leakage to the air reactor, as well as the flue gas contents of char and tar, should be as low as possible. Generally, the heating value of the cleaned product gas should be as high as possible. Not so surprisingly, black pellets and wood pellets, i.e., fuels with high volatiles content, are more suitable for chemical-looping gasification than wood char. During chemical-looping gasification with black pellets as fuel, the dry flue gas consisted mostly of H_2, followed by CO_2, CO, CH_4, and C_2-species, not counting N_2. This raw gas is suitable for further processing toward a desired product.

The following conclusions can be drawn from the investigation conducted:

- LD slag is an industrial by-product, which is available in huge quantities and for which there is currently a very limited demand. To be used as oxygen carrier in a chemical-looping process, essentially, only crushing is required. Therefore, it should be much cheaper to produce than oxygen-carrier materials based on minerals and ores.
- LD-slag-based oxygen carrier develops CLOU properties during the initial hours of fuel operation, i.e., about 85 redox cycles. During that period, its fuel conversion properties improve significantly.
- With LD-slag-based oxygen carrier, 99.9% conversion of CO to CO_2 is possible.
- With high-volatile fuels, i.e., black pellets and wood pellets, no C_3-hydrocarbons were detected in the fuel reactor fuel gas. With a low-volatile fuel, i.e., wood char, neither C_2- nor C_3-hydrocarbons were detected.
- Carbon leakage to the air reactor was low, in most cases below 1% of the fuel carbon, so that high carbon capture efficiencies should be feasible.
- During chemical-looping gasification operation with high-volatile fuels, i.e., black pellets and wood pellets, a raw gas was produced that contained mostly hydrogen and that should be feasible for further processing toward a desired gas blend.
- Based on fines production, the particle lifetime was estimated to be 110–170 h. In a conventional CFB combustor, this lifetime would correspond to a bed regeneration rate of about 5–8 kg/MWh, which is close to conventional regeneration rates and should, therefore, be feasible.

4.2 Global mitigation strategy recommendations

As explained in the introduction, there is no industrial development of the chemical-looping combustion process despite large expected cost reduction for CO_2 capture as well as other potential benefits.

Any policy properly addressing climate change will include a significant price on CO_2 emissions, as well as a substantial recompense for negative CO_2 emissions. Waiting for this to happen, it is very important to foster the development and up-scaling of the technologies that will be needed in future. The reason is the long time needed to go from typical small-scale pilots, e.g., 5 m high and 0.1 MW to the commercial scale, e.g., 50 m high and > 100 MW. To have the option to use this technology in the 2030s, the up-scaling needs to start now.

There are many financial instruments available that could achieve the demonstration of technologies where the market is presently not available. In the case of new technology like chemical-looping combustion, the policies would need to provide both adequate funding of the development and erection CO_2 capture facility, as well as stable financing of the operation of the CO_2 capture. Also, the cost of transportation and storage would need to be covered.

Here is a proposed example of such a policy. The European Emission Trading System, ETS, could be modified in such a way that, for instance, 0.5% of the fossil CO_2 emissions traded would need to be compensated by negative emissions and a certain share of this should be used for developing novel capture technologies for negative CO_2 emissions. The cost for this will be shared on all emission trade rights. An institution would be responsible for buying the negative emissions considering cost, as well as technology development aspects.

Acknowledgements The contribution of SSAB Merox AB in the preparation of LD slag is acknowledged.

Funding information This work was carried out as part of the OxyCar-FBC project, which is conducted within the framework of ERA-NET Bioenergy and funded by the Swedish Energy Agency (P43936-1). This project has received additional support from a grant of the Swedish Energy Agency (P43220-1).

References

Adánez J, Abad A, García-Labiano F, Gayán P, de Diego LF (2012) Progress in chemical-looping combustion and reforming technologies. Prog Energy Combust Sci 38(2):215–282

Berdugo Vilches T, Lind F, Rydén M, Thunman H (2017) Experience of more than 1000h of operation with oxygen carriers and solid biomass at large scale. Appl Energy 190:1174–1183

European Technology Platform for Zero Emission Fossil Fuel Power Plants (2011) The costs of CO_2 capture: post-demonstration CCS in the EU. Zero Emissions Platform: online: http://www.zeroemissionsplatform.eu/library/publication/166-zep-cost-report-capture.html. Accessed 3 March 2019

Haaf M, Ohlemüller P, Ströhle J, Epple B (2018) Assessment of the potential for negative co_2 emissions by the utilization of alternative fuels in 2nd generation CCS processes. In: International Conference on Negative CO_2 Emissions. Gothenburg, Sweden

Imtiaz Q, Hosseini D, Müller CR (2013) Review of oxygen carriers for chemical looping with oxygen uncoupling (CLOU): thermodynamics, material development, and synthesis. Energy Technol 1(11):633–647

Johnsson F, Vrager A, Leckner B (1999) Solids flow pattern in the exit region of a CFB-furnace - influence of exit geometry. In: Fifteenth International Conference on Fluidized Bed Combustion. Savannah, GA, USA, p 20

Källén M, Rydén M, Lyngfelt A, Mattisson T (2015) Chemical-looping combustion using combined iron/manganese/silicon oxygen carriers. Appl Energy 157:330–337

Keller M, Leion H, Mattisson T, Thunman H (2014) Investigation of natural and synthetic bed materials for their utilization in chemical looping reforming for tar elimination in biomass-derived gasification gas. Energy Fuels 28(6):3833–3840

Kunii D, Levenspiel O (1991) Fluidization engineering, 2nd edn. Butterworth-Heinemann, Boston, p 491

Lind F, Berguerand N, Seemann M, Thunman H (2013) Ilmenite and nickel as catalysts for upgrading of raw gas derived from biomass gasification. Energy Fuel 27(2):997–1007

Linderholm C, Lyngfelt A, Cuadrat A, Jerndal E (2012) Chemical-looping combustion of solid fuels - operation in a 10 kW unit with two fuels, above-bed and in-bed fuel feed and two oxygen carriers, manganese ore and ilmenite. Fuel 102:808–822

Linderholm C, Schmitz M, Biermann M, Hanning M, Lyngfelt A (2017) Chemical-looping combustion of solid fuel in a 100kW unit using sintered manganese ore as oxygen carrier. Int J Greenhouse Gas Control 65:170–181

Lyngfelt A, Leckner B (2015) A 1000 MW_{th} boiler for chemical-looping combustion of solid fuels – discussion of design and costs. Appl Energy 157:475–487

Lyngfelt A, Leckner B, Mattisson T (2001) A fluidized-bed combustion process with inherent CO_2 separation; application of chemical-looping combustion. Chem Eng Sci 56:3101–3113

Lyngfelt A, Mattisson T, Rydén M, Linderholm C (2018) 10,000 h of Chemical-looping combustion operation – where are we and where do we want to go? In: 5th International Conference on Chemical Looping. Park City, UT, USA

Moldenhauer P, Sundqvist S, Mattisson T, Linderholm C (2018a) Chemical-looping combustion of synthetic biomass-volatiles with manganese-ore oxygen carriers. Int J Greenhouse Gas Control 71:239–252

Moldenhauer P, Serrano A, García-Labiano F, De Diego LF, Biermann M, Mattisson T, Lyngfelt A (2018b) Chemical looping combustion of kerosene and gaseous fuels with a natural and a manufactured Mn-Fe-based oxygen carrier. Energy Fuel 32(8):8803–8816

Rydén M, Leion H, Mattisson T, Lyngfelt A (2014a) Combined oxides as oxygen-carrier material for chemical-looping with oxygen uncoupling. Appl Energy 113:1924–1932

Rydén M, Moldenhauer P, Lindqvist S, Mattisson T, Lyngfelt A (2014b) Measuring attrition resistance of oxygen carrier particles for chemical looping combustion with a customized jet cup. Powder Technol 256:75–86

Schmitz M, Linderholm C, Hallberg P, Sundqvist S, Lyngfelt A (2016) Chemical-looping combustion of solid fuels using manganese ores as oxygen carriers. Energy Fuels 30(2):1204–1216

Wang P, Leion H, Yang H (2017) Oxygen-carrier-aided combustion in a bench-scale fluidized bed. Energy Fuels 31(6):6463–6471